HiSST: International Conference on
High-Speed Vehicle Science & Technology
26–29 November 2018, Moscow, Russia

Experimental Investigation on Flight Test Vehicle Aerodynamics at TsAGI T-116 Wind Tunnel: Powered and Glider Options

Anatoly A. Gubanov[1], Dmitry Yu. Gusev[2], Valentina A. Yakovleva[3]

Abstract

The results of experimental investigation on aerodynamics of the two experimental flight test vehicle EFTV options (powered and glider ones) which are under study within the international project HEXAFLY-INT are presented. The tests were performed in TsAGI supersonic and hypersonic wind tunnel T-116 at Mach numbers from 3 to 8. Particular attention is paid to aerodynamic efficiency and trim-ability of the vehicles. It is shown that at Mach number M = 7 maximum aerodynamic efficiency of both the EFTV powered option with started intake and the glider option is of approximately the same value $(L/D)_{max} \approx 4.5$, and problems with trim-ability on pitch occur just for the powered option if the intake is not started.

Keywords: *aerodynamics, experimental investigation, wind tunnel, experimental flight test vehicle*

Nomenclature

Abbreviations:
BL – boundary layer
EFTV – experimental flight test vehicle
ESM – experimental service module
MRC – moment reference centre

Latin symbols:
A – axial force
C – aerodynamic force or moment coefficient
CR – contracting ratio
D – top diameter of the screw head
d – diameter of the wire
F – area
f – intake air mass flow rate coefficient
H – flight altitude
I – momentum
k – height
L– length of the model fuselage
L/D – aerodynamic efficiency
M – Mach number; aerodynamic moment
P – pressure
Re– Reynolds number
S – area
T – temperature
V – velocity

[1]*Central Aerohydrodynamic Institute n.a. prof. N.E. Zhukovsky (TsAGI),140180, Zhukovsky str. 1, Zhukovsky Moscow region, anatoly.gubanov@tsagi.ru*
[2]*Central Aerohydrodynamic Institute n.a. prof. N.E. Zhukovsky (TsAGI),140180, Zhukovsky str. 1, Zhukovsky Moscow region, ddgg@progtech.ru*
[3]*Central Aerohydrodynamic Institute n.a. prof. N.E. Zhukovsky (TsAGI),140180, Zhukovsky str. 1, Zhukovsky Moscow region, valentinayakovleva@list.ru*

Greek symbols:
α – angle-of-attack
Δ – arm; methodological correction
δ – flap deflection angle
ρ – density

Subscripts:
D – related to drag force
G – related to the EFTV glider option
L – left; related to lift force
m – related to pitching moment
N – related to the nozzle exit
P – related to the EFTV powered option
R – right
ref – characteristic value
tot – total
0 – related to the intake entrance area
$1m$ – defined for the length of 1 m
∞ – related to free-stream condition

I. Introduction

The paper presents the main results of experimental study on aerodynamics of the two options of the high-speed Experimental Flight Test Vehicle (EFTV) which are under study within the International Project HEXAFLY-INT. The Project with partners from Europe, Russian Federation and Australiais aimed at study of several technologies related to the Mach 8 LAPCAT-MR2 hydrogen-fueled passenger vehicle concept (Fig. 1) which had been developed within the European Project LAPCAT II [1]. The main features of the aerodynamic configuration of the LAPCAT-MR2 vehicle are waverider-shaped wing and the streamline-traced intake with an elliptical entrance located in dorsal position at the forward part of the fuselage.

Fig.1LAPCAT-MR2 vehicle

Both options of the EFTV vehicle of approximately 3 m length each had been developed for flight tests with use of the Brazilian sounding rocket VS 43. The qualitative flight-test scenario for the EFTV vehicle taken from Ref. [2] is shown on Fig. 2.

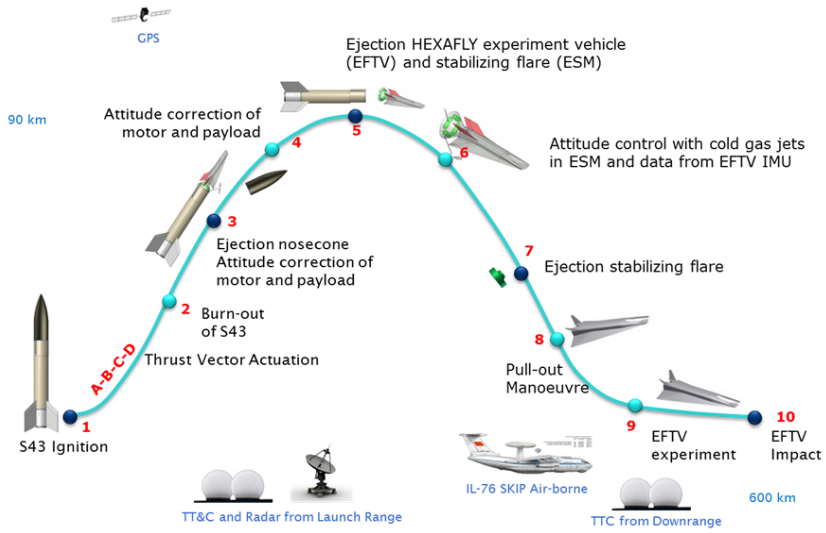

Fig. 2HEXAFLY-INT qualitative mission scenario

Configuration of the powered option of the test vehicle shown on Fig. 3 (left) had been developed within the preceding European Project HEXAFLY [3]. Its geometry is similar to that of the full-scale LAPCAT-MR2 vehicle including the streamline-traced intake [4]. External configuration of the EFTV glider option was developed within the currently ongoing International Project HEXAFLY-INT by placing the nose cap in the forward part of the vehicle instead of the intake entrance. The EFTV glider is intended to undergo flight tests at the final stage of the Project. Its configuration is shown on Fig. 3 (right) connected with the Experimental Service Module (ESM) which will be used for controlling the vehicle attitude during the descent phase of the flight-test trajectory and detached from the EFTV vehicle before the pull-out maneuver and the gliding phase.

Fig.3 EFTV vehicle options: powered (left) and glider with ESM (right)

For wind-tunnel tests in supersonic and hypersonic wind tunnel T-116 having the working chamber with the squared cross-section of 1 m × 1 m size, TsAGI designed and produced aerodynamic model of the EFTV vehicle with the scale 0.35 related to the size of the real flight-test vehicle in order to fit the wind-tunnel requirements – the model should be of about 1 m length. The model allowed investigating both options of the EFTV vehicle without ESM by change of its nose and aft parts. The model of powered option was made with the internal duct in order to study the intake characteristics and to take into account the influence of the air passage through the engine including the influence of the compressed flow spillage before the intake entrance on the external aerodynamics of the vehicle. For simulating the glider configuration, the intake was replaced by the nose cup, and the aft part of the model was simplified by closing the nozzle of the duct.

The model was made with possibility of providing tests both without flap deflection and with deflection of right and left flaps individually or in different combinations by angles $\delta_{R,L}$ = ±6°, ±12° and ±18°.

The values of the plan-form area of the EFTV powered option model is S_P = 0.2989 m^2, and that of the glider model S_G = 0.3087 m^2. These values were used as the characteristic area S_{ref} of models for calculating coefficients of aerodynamic force and moment components. For calculating the pitching moment coefficient, the length of the model fuselage for the EFTV powered option from the leading edge to the base section L_P = 1.0066 m was used as the characteristic length L_{ref}. Similarly, the value L_G = 1.15 m was used as the characteristic length for the glider model. Positions of the moment reference center (MRC) for both EFTV options are shown on Fig. 4. The intake entrance area of the powered option model used as the characteristic area for calculating the intake mass flow rate coefficient was F_0 = 0.005131 m^2.

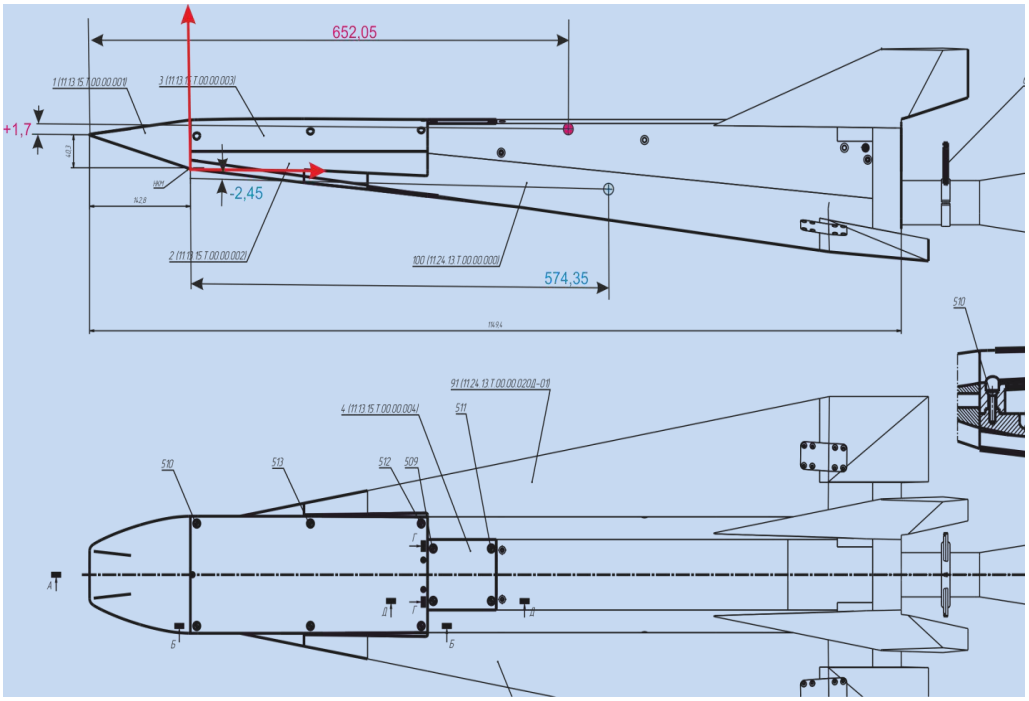

Fig. 4 Positions of the MRC for powered (blue) and glider (red) EFTV options

II.Aerodynamic Investigation on the EFTV Powered Option

Aerodynamics of the powered option of the EFTV vehicle is under study within the HEXAFLY-INT project by CFD and ground tests just by Russian partners. Composition of the powered option model and the photo of the model installed in the working chamber of T-116 are presented on Fig. 5.

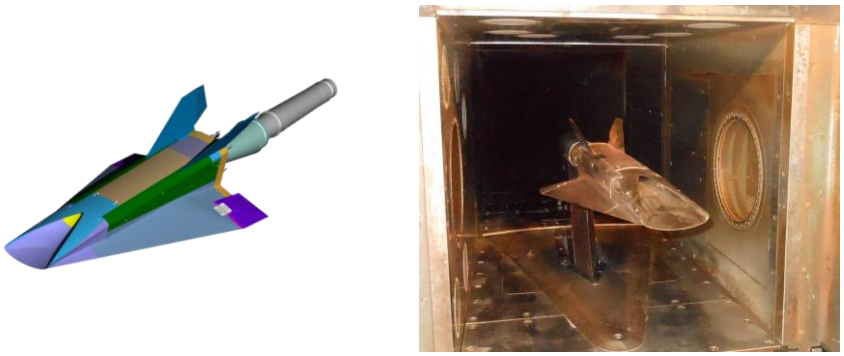

Fig. 5 Composition and photo of the EFTV powered option aerodynamic model

The internal duct of the model was made with the "sonic" exit nozzle in order to provide rather precise measurement of the exit flow parameters during tests by the special rake containing several total and static pressure probes and thermocouples. The results of measurement were used for calculating both the intake mass flow rate coefficient and the exit flow momentum for introducing the necessary corrections to the experimental data. Longitudinal section of the model showing the shape of the internal flow path, the tail sting, and the measurement rake is presented on Fig. 6. In order to

study the influence of the intake throat area on the starting of the intake, the model was made with two variants of the intake throat inserts showed on Figs. 5 and 6 by yellow colour: the first one corresponding to the original intake contracting ratio CR = 8.6, and the second one having the widened throat CR = 7.4, without internal contracting of the channel after the section of the intake crotch.

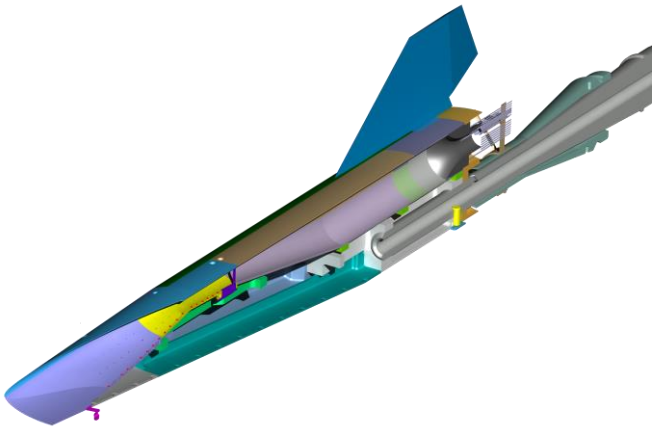

Fig. 6 Longitudinal section of the model

Aerodynamic characteristics of the model were determined by measurement of aerodynamic force and moment components during the tests by the electromechanical balance, with introducing the necessary methodological corrections including corrections on deformation of the tail sting, base drag correction, and the correction on internal aerodynamic force and moment. Deformation of the tail sting was measured by special calibration. The base drag correction resulted in reducing the pressure on the base section of the model to the value of static pressure in the free stream. According to the methodology adopted in Russian Federation [5], correction on the internal force was made just for the axial force component in the body reference frame so as to simulate the condition of the nozzle exit flow momentum equality to the initial momentum (in the free-stream area) of the stream tube passing through the internal duct of the model. For making it, the values of the nozzle exit flow momentum I_N and of the intake mass flow rate coefficient f were determined by calculations from the results of measurement the exit flow parameters by the measurement rake, and the difference between the initial momentum of the stream-tube passing through the internal duct I_∞ and the exit flow momentum I_N subtracted from the results of measurement the axial force A acting on the model by the balance:

$$\Delta A = -(I_\infty - I_N).$$

The value of I_∞ is determined by the formula

$$I_\infty = \rho_\infty V_\infty^2 F_0 f,$$

ρ_∞ and V_∞ are values of density and velocity in the free stream, F_0 is the intake entrance area which is used for determination the intake mass flow rate coefficient f.

Correction for the pitching moment M_m is determined by the formula

$$\Delta M_m = -\Delta A \cdot \Delta z,$$

Δz is the arm of the exit nozzle axis, the absolute value of which is measured as a distance between the nozzle axis and the adopted moment reference centre (MRC) position; the sign of Δz is chosen to be positive if the nozzle axis goes above the MRF.

Experimental study of aerodynamic performance of the model had been performed in TsAGI supersonic and hypersonic wind tunnel T-116 at Mach numbers M = 7 and 8 with Reynolds numbers fairly corresponding to those of the intended flight-test condition: Re_{1m} = $7.66 \cdot 10^6$ (the corresponding altitude of the EFTV vehicle flight is H = 30 km) and $5.92 \cdot 10^6$ (H = 31.5 km) accordingly. Additionally, one test was conducted at Mach number M = 7 with lower Reynolds number Re_{1m} = $4.22 \cdot 10^6$ (H = 34 km).

The experimental results presented earlier in Ref. [2] showed that the intake starting significantly depends on both the contracting ratio of the intake CR and the presence of flow disturbances before the intake entry. The first test series of the model showed that start of the intake with smooth internal surface (without any disturbance generators) in T-116 took place just with the expanded throat (CR = 7.4) at M = 8 and negative angles-of-attack $\alpha \leq$ - 1°. At lower Mach numbers the intake did not start at all. It was supposed that the start of the intake depends from the boundary layer (BL) state on the intake compression surface, and the second series of tests was provided with different transition grits installed on the intake surface in the vicinity of its leading edge. Shapes of the four different transition grits used in the second test series are shown on Fig. 7. The 1st variant of transition grit consisted of 2 metallic strips with 3 rows of diamond-shaped roughness elements each; the heights of the roughness elements were 0.75 mm and 1 mm, the 2nd variant consisted of 10 "dovetail" heads of M2 screws having the height k = 1.2 mm and the top diameter D = 3.8 mm, 2 screws being located in the symmetry plane of the intake and 2 couples being placed both to the left and to the right of it, the 3rd and the 4th variants of transition grits were represented by the same screw heads with wires of the diameter d = 0.5 mm attached to the model surface by the screws in "cross" position (variant 3) and in "lines" position, in parallel to the intake leading edge (variant 4).

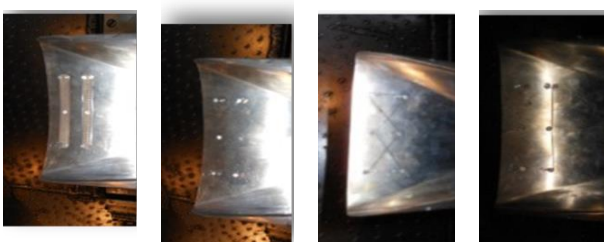

Fig. 7 Different variants of the BL transition grits used in the second test series

Positions of the screw heads installed on the intake surface for variants of transition grits from 2 to 4 are shown on Fig. 8.

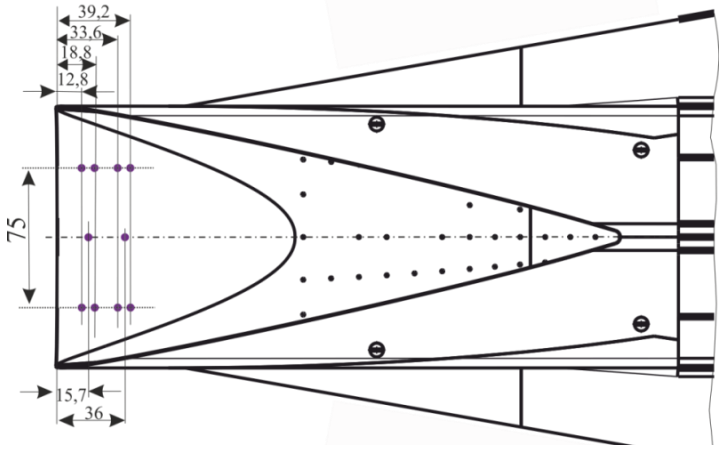

Fig. 8 Positions of screw heads installed on the intake surface (variants from 2 to 4)

The results of tests in terms of the intake mass flow rate f dependences from angle-of-attack of the model α obtained at Mach numbers 8 and 7 at different flow conditions are shown on Fig. 9. It is seen that installing of transition grits led to significant change of the intake starting behaviour: the variant 1 of transition grit destroyed intake starting even at M = 8 and negative angles-of-attack, while variants from 2 to 4 led to significantly wider ranges of test conditions at which the intake was started. It was observed that at M = 7 the intake mass flow rate coefficient diminishes with the Reynolds number decrease. As further investigation showed, the variant 2 of transition grit allowed getting the intake started also at M = 6.

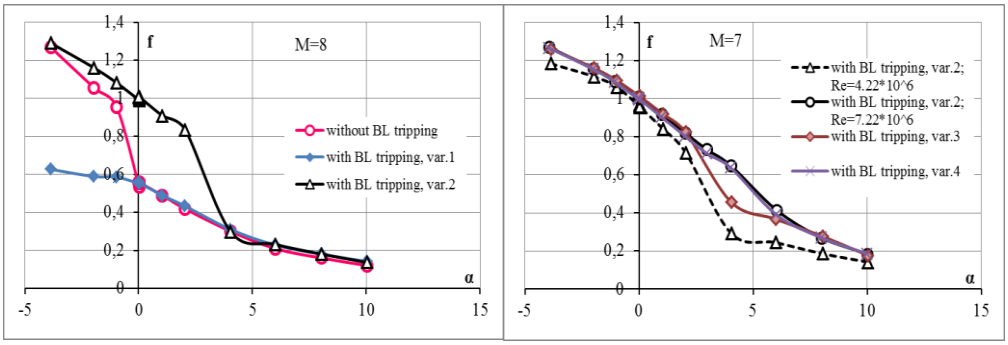

Fig. 9 The intake mass flow rate coefficient f vs. angle-of-attack of the model α

External aerodynamic characteristics of the model were investigated at Mach numbers M=8 and 7 with and without transition grit variant 2. The results of tests in terms of drag and lift force coefficients C_D and C_L, aerodynamic efficiency L/D and pitching moment coefficient C_m of the model without flap deflection are presented on Figs. 10 and 11.

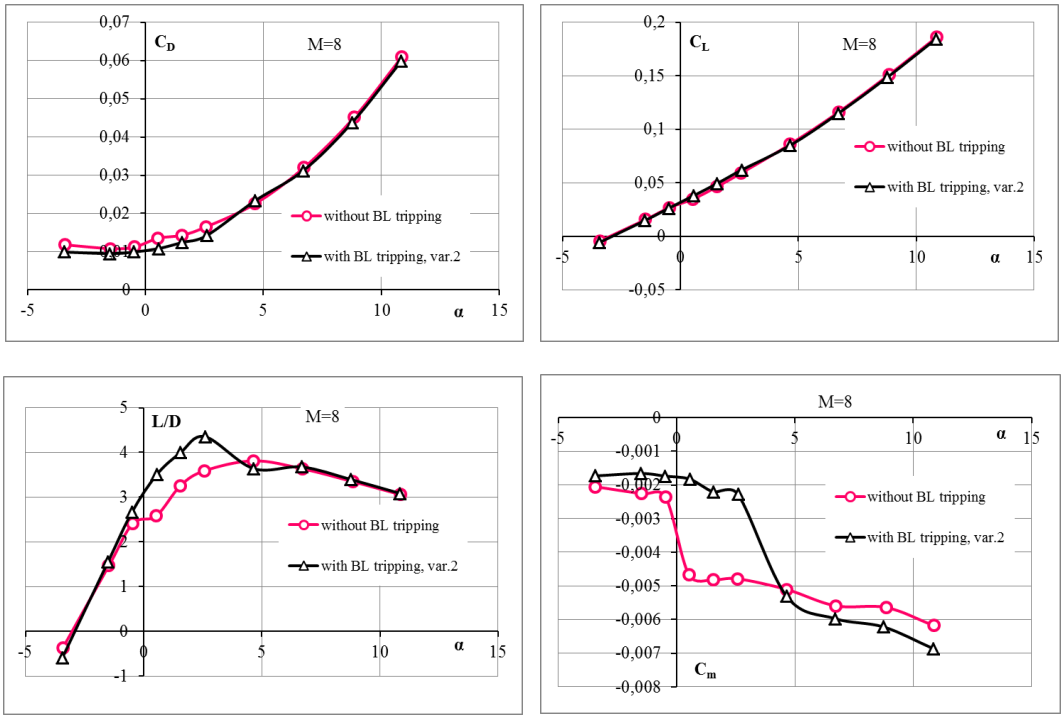

Fig.10 Drag and lift force coefficients C_D and C_L, aerodynamic efficiency L/D and pitching moment coefficient C_m vs. angle-of-attack of the model α. M = 8, δ = 0

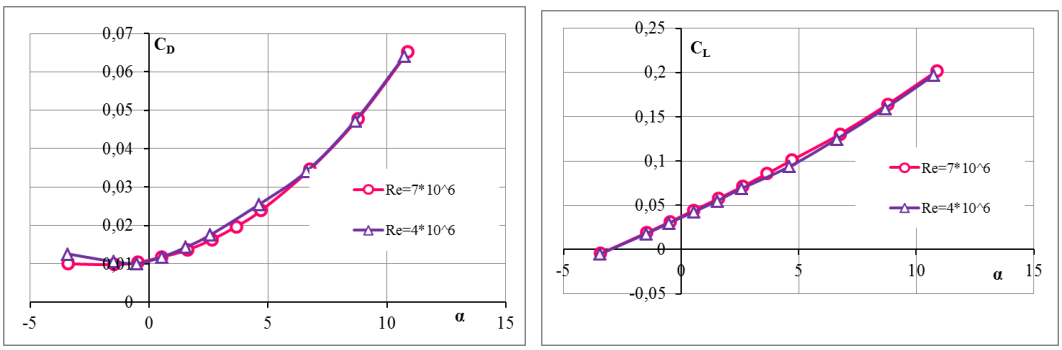

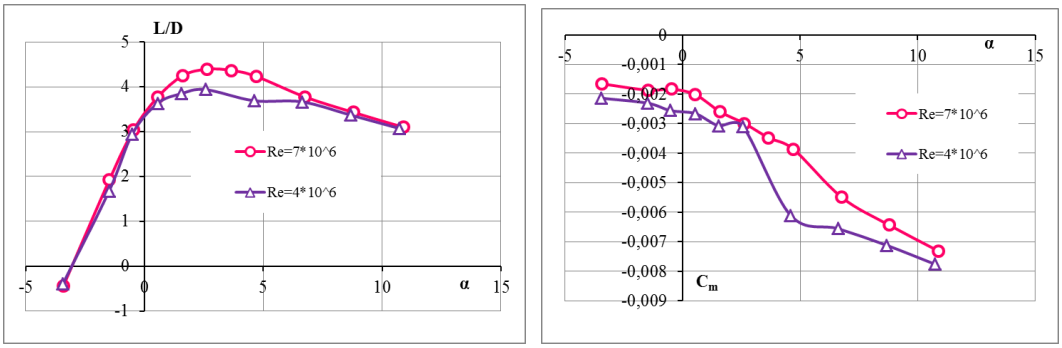

Fig.11 Drag and lift force coefficients C_D and C_L, aerodynamic efficiency L/D and pitching moment coefficient C_m vs. angle-of attack of the model α. M = 7, transition grit variant 2, δ = 0

It is seen that both the drag force and the pitching moment of the model depend on the intake starting dramatically: at angles-of-attack at which the intake unstarts, large increment of the drag force consisting of approximately 20 % of the total drag force of the vehicle appears due to spillage of compressed flow before the intake entry, and tremendous value of additional negative pitching moment occurs.

The results of tests obtained at M = 7 on the model with different symmetrical flap deflections are presented on Fig. 12.

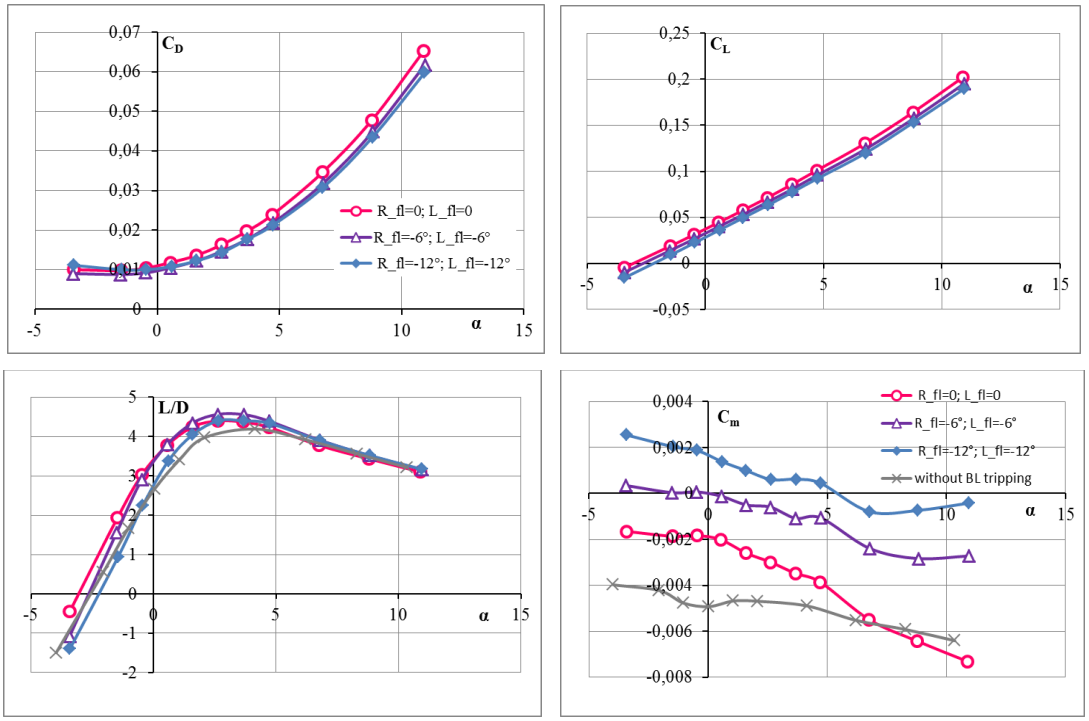

Fig. 12 Drag and lift force coefficients C_D and C_L, aerodynamic efficiency L/D and pitching moment coefficient C_m vs. angle-of attack α. M = 7, transition grit variant 2 with different right (R_fl) and left (L_fl) flap deflection, and without transition grit,R_fl = L_fl = 0

It is seen that the maximum value of aerodynamic efficiency $(L/D)_{max}$of the EFTV vehicle with the transition grit variant 2 at M = 7 is about 4.5, and the vehicle can easily be trimmed on pitch at angles-of-attack up to 5° – with flap deflections not exceeding 12° by absolute value. The model without transition grit displays the value of $(L/D)_{max} \approx 4.1$, and its trimming on pitch becomes problematic within the considering range of flap deflection angles.

III. Experimental investigation on the EFTV glider option aerodynamics

The glider option of the EFTV vehicle will be tested in free-flight condition within the current HEXAFLY-INT Project, and its aerodynamics is studying by European, Russian and Australian

Partners.The photo of the aerodynamic model for glider option is shown on Fig.13. The test results of the glider model were presented in Ref. [6].

Fig.13 The model for tests of EFTV glider in T-116

The model was tested in T-116 within the Mach number range from 3 to 8. The flow parameters realized during the tests are presented in Table 1. The table indicates the values of Mach number M, total pressure P_{tot}, total temperature T_{tot}, Reynolds number Re_{1m} calculated for the length of 1 m, and the corresponding flight altitude H for the EFTV vehicle. In terms of the Reynolds number, the test conditions in T-116 are reasonably close to those expecting during the flight test of the vehicle.

Table 1 The flow parameters realized in T-116 during tests of the glider model

M	3.03	4.05	5.05	6.00	6.99	7.88
P_{tot}, atm	1.1	1.4	5.0	7.4	22.0	31.5
T_{tot}, K	300	300	455	485	675	825
$Re_{1m}*10^{-6}$	7.74	5.96	6.88	6.32	7.66	5.92
Simulated Flight Altitudes for the EFTV vehicle:						
H, km	24.8	28.0	28.4	30.5	30.0	32.5

The main aerodynamic characteristics of the glider model (without flap deflection) in terms of aerodynamic drag force coefficient C_D, aerodynamic efficiency L/D, and pitching moment coefficient C_m vs. angle-of-attack α with zero sideslip angle are presented on Fig. 14.

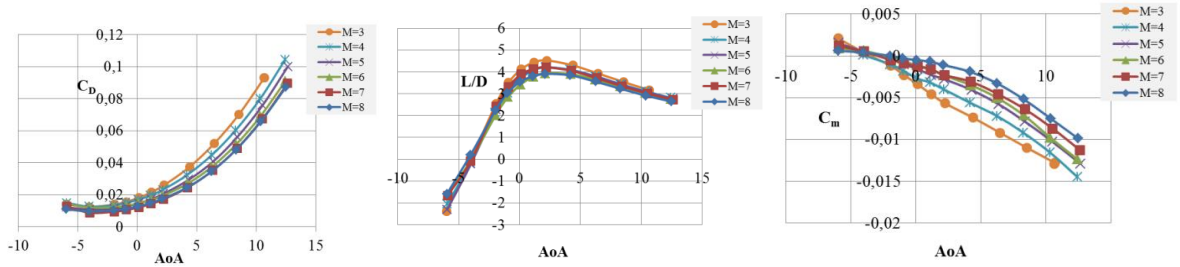

Fig.14 Drag force coefficients C_D, aerodynamic efficiency L/D and pitching moment coefficient C_m of the glider vs. angle-of attack α. δ = 0

It is seen from the figure that maximum values of aerodynamic efficiency of the model change from 4.5 to 4.0 with the Mach number increase from 3 to 8, and stability of the model on pitch also diminishes. Comparison with the experimental data for the EFTV powered option model shows that the input of the nose cap of the glider model into aerodynamic drag force of the vehicle is of the same order as the sum of the drag force related to the leading edges of the intake and the intake spillage drag at started condition.

The pitching moment coefficient of the model C_m dependences from angle of symmetrical deflection of both flaps within the range δ = –18°…+6° at Mach numbers 4 and 7 and different angles-of-attack are shown on Fig.15.

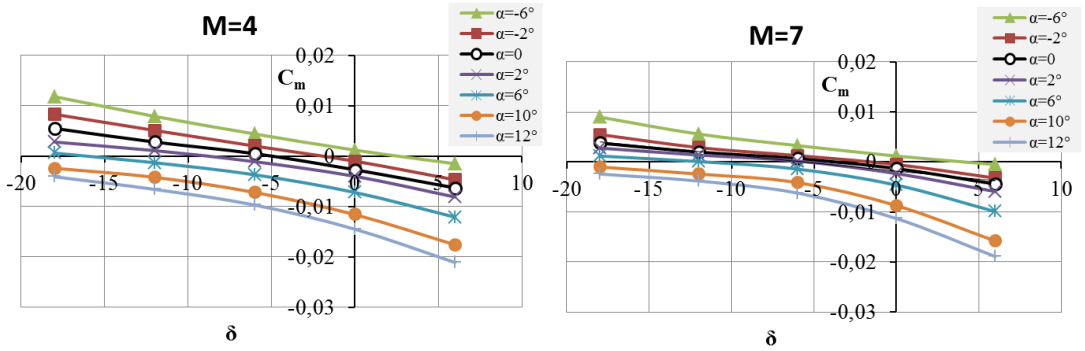

Fig.15 Pitching moment coefficient of the glider model C_m vs. flap deflection angle δ

It is seen from the figure that the EFTV glider with the considering MRC position can be trimmed on pitch at angle-of-attack range from –6° to +6° by flap deflection from +2.5° to –16° at Mach number M = 4, and from +4° to –12° at M = 7.

IV. Conclusion

1. The results of experimental investigation on EFTV powered option aerodynamics showed that if the intake starts, the maximum aerodynamic efficiency of the vehicle at Mach number M = 7 is of about 4.5, and it can easily be trimmed on pitch at angles-of-attack up to 5° by flap deflection angles of absolute values less than 12°.
2. In case if the intake unstarts, considerable increments in drag force and pitching moment occur, which lead to diminution of maximum lift-to-drag ratio to 4.1, and the trimming of the vehicle on pitch becomes problematic.
3. Maximum values of aerodynamic efficiency of the EFTV glider model change from 4.5 to 4.0 with the Mach number increase from 3 to 8, and stability of the model on pitch also diminishes.
4. Comparison of the experimental data on aerodynamics of the two EFTV options shows that the input of the nose cap of the glider into aerodynamic drag force of the vehicle at M = 7 is of the same order of magnitude as the sum of the drag force related to the leading edges of the intake and the intake spillage drag at started condition.
5. With the considering position of the moment reference centre, the chosen configuration of flaps allows for the EFTV glider to be trimmed on pitch at angles-of-attackrange from –6° to +6° by flap deflection from +2.5° to –16° at Mach number M=4, and from +4° to –12° at M=7.

References

1. Steelant, J., Varvill, R., Defoort, S., Hannemann, K., and Marini, M.: Achievements Obtained for Sustained Hypersonic Flight within the LAPCAT-II project. 20th AIAA International Space Planes and Hypersonic Systems and Technologies Conference, Glasgow Scotland, July 6-9, 2015: AIAA-2015-3677.
2. Steelant, J., Villace, V., Marini, M., Pezzella, G., Reimann, B., Chernyshev, S., Gubanov, A., Talyzin, V., Voevodenko, N., Kukshinov, N., Prokhorov, A., Neely, A., Kennell, C., Verstraete, D., Buttsworth, D.: Numerical and Experimental Research on Aerodynamics of High Speed Passenger Vehicle within the HEXAFLY-INT Project. 30th Congress of International Council of the Aeronautical Sciences (ICAS), Daejeon Korea, September 25-30, 2016.
3. Steelant, J., Langener, T., Di Matteo, F., Hannemann, K., Riehmer, J., Kuhn, M., Dittert, C., Scheuerpflug, F., Jung, W., Marini, M., Pezzella, G., Cicala, M., Serre, L.: Conceptual Design of the High-Speed Propelled Experimental Flight Test Vehicle HEXAFLY. 20th AIAA International Space Planes and Hypersonic Systems and Technologies Conference, Glasgow Scotland, 6-9 July 2015: AIAA-2015-3539.
4. Meerts, C., Steelant, J.: Air Intake Design for the Acceleration Propulsion Unit of the

LAPCAT-MR2 Hypersonic Aircraft. 5th European Conference for Aeronautics and Space Sciences (EUCASS), Munich Germany, July 1-5, 2013.
5. Blishch, V.G.: External and internal aerodynamic forces and moments of air-breathing jet powered vehicles and their models at incidence and sideslip. Trudy TsAGI, 1987, Issue 2328 (in Russian).
6. Marini, M., Pezzella, G., Schettino, A, Di Benedetto, S., Fernandez-Villace, V., Steelant, J., Gubanov, A., Voevodenko, N., Reimann, B., Walton, C.: Numerical and Experimental Aerodynamic Characterization of the HEXAFLY-INT Hypersonic Glider. 21st AIAA International Space Planes and Hypersonic Systems and Technologies Conference, Xiamen China, March 6-9, 2017: AIAA-2017-2316.